Proceedings World Geothermal Congress 2020+1
Reykjavik, Iceland, April - October 2021

Corrosion Testing in Direct Geothermal Steam of Cladded and Standalone Materials at 210°C and 450°C

Ingolfur O. Thorbjornsson[1], Bente C. Krogh[2], Gunnar S. Kaldal[1], Gisle Rørvik[2], Sigurdur S. Jonsson[1], Larus Gudmundsson[1], Finnbogi Oskarsson[1], Omar Sigurdsson[3], Hans Husby[2], Arni Ragnarsson[1]

[1] Isor-Iceland Geosurvey, Grensásvegur 9, 108 Reykjavik

[2] Equinor ASA, Arkitekt Ebbels veg 10, 7005 Trondheim, Norway

[3]HS-Orka, Svartsengi, 240 Grindavik

Ingo@isor.is

Keywords: geothermal corrosion, superheated steam, corrosion resistant materials, cladded materials, GeoWell

ABSTRACT

Selection of materials for high-temperature geothermal wells follows oil and gas (O&G) standards and recommendations and the same applies for wellhead design, well design and drilling. Geothermal wells differ from O&G wells with higher temperatures and often low pH level that enhance effects of non-condensable gases such as H_2S and CO_2. These are all parameters that have corrosive effect on the well material and often with more complicated forms of corrosion than in common O&G wells. It is therefore of high importance for long life of geothermal wells to select casing materials that can both withstand the high temperature and the corrosive nature of the geothermal fluid. The test was carried out at temperatures of 210°C and 450°C in a flow through system to test the corrosive nature of the geothermal environment against candidate materials, especially cladded materials made with several cladding methods. The cladded corrosion resistant alloys (CRA), cladded on low or medium carbon steels, were in direct contact with the steam/brine at a wellhead temperature 210°C, and further heated to 450°C, at Reykjanes geothermal field well RN 35 that is operated by HS Orka. The autoclave system for the testing is composed of three autoclaves, one 5 L and two smaller for sampling, made of C276 material and capable of providing testing conditions up to 450°C at 300 bars. Additionally, a custom-made autoclave was built for testing in direct conditions at 210°C.

1. INTRODUCTION

For material suitable for use in the geothermal industry, scientists and material providers have actively been looking into the corrosion nature of geothermal steam and brine for many years. This has resulted in better material selection for geothermal use, mainly in the surface equipment like valves, steam separators, pipes and not least in the turbines. More recently the focus has been moving over to the wells, traditionally designed according to O&G standards with respect to materials. In this paper, the focus will be on testing in an autoclave system where geothermal steam is directly used in a flow through system. The corrosive nature of the geothermal steam/brine is highly site dependent; the corrosive aggressiveness of geothermal fluids can vary from sour wells in volcanic sites to dry wells in older geothermal systems. The effect of non-condensable gases is of high importance, especially the partial pressure of H_2S that can trigger material cracking as Hydrogen Induced Cracking (HIC) or as SSC (Sulphide Stress Cracking). Beside the effect of low pH and amount of gases, free halogens such as Chloride (Cl^-) can trigger pitting corrosion and general corrosion. Here autoclave system constructed to be transportable from one well to another or from one field to another for in-situ testing was utilized. For the first time the behaviour of corrosion and as well scaling was studied at high temperature in the same geothermal steam at real conditions and compared to well head conditions. Material selection for a given well is clearly not a straight forward task, as it must be based on the site-specific conditions. Today the selection is based on API (American Petroleum Institute) and NACE (National Association of Corrosion Engineers) standard and guidelines of materials, selected for Oil and Gas wells. The materials that are most common are medium or low carbon steels and in most cases these material grades have proven to be successful. Today many wells with these materials have been in operation for over 30 years. Going into deeper and higher temperature fields generate furthermore increased interest in the materials as the more aggressive fluid in deeper geothermal sites calls for more resistant material solutions. Methods for cladding corrosion resistant materials on low or medium carbon steels include spraying, welding, explosion cladding and directly extruded pipes. In this paper selection of those methods was reported for the same steam conditions at 210°C and 450°C.

2. TEST SETUP

Within the GeoWell project it was decided to design and construct mobile test facility with an autoclave system to enable direct use of geothermal steam at elevated temperatures. Early stages of the development of the test-site facilities at Reykjanes high-temperature geothermal field included the construction of a suitable and sheltered housing with relatively easy access near electrical connections. HS-Orka supervised the construction and fitting of a ready-made 20’ office container. The container was divided in two separate rooms, with a reinforced explosion retarding dividing wall. The smaller room (approx. 30% of total floor area) was with an access door and work bench, electric space-heater, ventilation vents and specially constructed support table to which the autoclave, sampling test-vessel and associated coolers were securely bolted. The larger room had a separate access door and was intended to host all measuring equipment and computers, outfitted with ventilation, electrical space-heater and work bench.

Figure 1: Sampling point used as a steam source.

Sampling/connection point was selected further downstream on the steam pipe. The 1” valve/sampling point was located on the high-side of the steam pipe, approximately 25 m from the well-head as shown in Figure 1. From this point, gravitationally separated steam could be anticipated, and relatively dry steam would be obtained, without the operation of a Webre steam-separator. A sample taken from a condensate fluid from the sampling point yielded conductivity of 65 µS/cm at 25°C, confirming good separation of steam and brine at the location.

The system was connected to the sampling point valve using a thick wall 3/8” (OD) stainless pipe, insulated with a 25 mm glass-wool and aluminium outer protection coating. The other end of the pipe (~ 4m) was connected to a vessel designed by ISOR and manufactured by HS-Orka shown in Figure 2, intended to contain one set of the corrosion samples. Pressure and thermometer probes were installed on one end of the vessel. After pressure and performance testing the prepared samples were placed inside the outer vessel and it was closed and thoroughly insulated.

Figure 2: Outer experiment vessel, working at steam-pipe pressure and temperature.

After passing through the outer vessel, the steam was piped into the laboratory inside the container (Figure 4). A by-pass circuit had been constructed to flush out the piping before diverting the steam through the autoclave. A needle valve (control valve) was located at the input connection. At the bottom of the autoclave another needle valve was located. The third needle valve was located at the top of the autoclave to restrict the steam flow, in the event that the set temperature (450°C) could not be maintained, due to high flow of steam through the autoclave.

Figure 3: Insertion of samples in the outer vessel.

Samples to be submitted to the test in both “normal” temperature of the production well and elevated thermal conditions in the autoclave, were selected and placed in both test chambers.

Figure 4: Side view of autoclave for testing at 450°C, support table and pipework. The needle valve near the wall, leading from the top of the autoclave, restricted the outflow of steam to maintain constant temperature and control effective heating.

3.0 STEAM COMPOSITION

Before starting the corrosion testing, a steam sample was collected at the wellhead of RN-35, at a pressure of 29.2 bar-g. Sample fractions were collected for the analyses of all major gases in steam (CO_2, H_2S, H_2, N_2, O_2, Ar, CH_4) and selected volatiles (NH_3, B) and non-volatiles (Cl, Na) in condensate. The pH and electrical conductivity of the condensate were also determined.

The steam sample for gas analysis was collected to a double-port glass flask, containing 50 mL of 10 M NaOH, but otherwise evacuated. When collecting condensate samples, steam was condensed and cooled to ambient temperature in a stainless-steel cooling spiral and the condensate collected to amber glass bottles (for volatile analyses) and LDPE bottles (for B and non-volatiles). The sample collection procedure is discussed in greater detail by Arnórsson et al. (2006).

The chemical composition of the steam and condensate is given in Table 1. The liquid phase (brine) of the well discharge was sampled at the same day and same pressure. Its composition is not relevant for this study, but it should be noted that it has high salinity; total dissolved solids, determined by dry evaporation, amount to 42,000 mg/kg solution – of which Cl is 24,300 mg/kg, Na is 12,200 mg/kg, and SiO_2 is 820 mg/kg; and a room temperature pH of 5.50.

Table 1: Chemical composition of steam collected from well RN-35 on 16 October 2018. Concentrations are given as mg/kg in steam.

Component	Concentration
GAS IN STEAM	
CO_2	5,620
H_2S	235
H_2	0.67
N_2	71.4
O_2	<0.01
Ar	2.02
CH_4	1.61
CONDENSED STEAM	
pH	4.06 / 22°C
Conductivity (µS/cm)	138 / 25°C
NH_3	3.14
B	0.51
Cl	16.3
Na	5.51

The gas concentrations are within the range that has been observed for two-phase wells in the Reykjanes system (Óskarsson et al., 2015). From the electrical conductivity and sodium concentration in condensed steam, it is apparent that the sample is somewhat affected by brine carryover. The conductivity of a well-separated steam condensate in Reykjanes is typically on the order of 50-70 µS/cm, and sodium is usually less than 1 mg/kg. The sodium concentration may be used to calculate the separation efficiency (steam quality) according to:

$$X = \left(1 - \frac{Na_{steam}}{Na_{brine}}\right)$$

which yields a separation efficiency of 99.95%.

The associated further boiling of the two-phase fluid results in gas concentrations which are significantly lower than at the wellhead pressure. The geochemical speciation program WATCH (Arnórsson et al., 1982; Bjarnason, 2010), was used to calculate the concentrations of gas in steam after adiabatic boiling to 20 bar_g. The resulting concentrations are given in Table 2.

Table 2: Concentrations of gas in steam from well RN-35 after boiling to 20 bar_g. Concentrations are given as mg/kg steam.

Component	Concentration
CO_2	4,430
H_2S	182
H_2	0.52
N_2	55.9
O_2	<0.01
Ar	1.49
CH_4	1.26

4.0 MATERIALS

4.1 Sample holders and list of samples

For testing, both in the test chamber outside the container and in the autoclave setup inside the container, identical sample holders were designed and constructed. Mesh screens were used for centralization and alumina ceramic collars and washers for insulation. Figure 5 shows the test coupons listed in Table 3.

Material selection was based on the knowledge given by earlier studies of corrosion resistance of material tested in high temperature geothermal steam (Thorbjornsson, 2015; Karlsdottir, 2013). For collecting materials, several material producers were contacted and those able to send samples of their materials, cladded and stand-alone, were selected for the testing. Materials were obtained from Butting, Explomet, Indosteel, Sandvik, Haynes International and Timet. Material was also gathered from Sintef (www.Sintef.no) and the Icelandic national power company Landsvirkjun (www.lv.is).

Figure 5: Assembled sample holders and position of samples listed in Table 3. The setup of both sample holders, for testing in 210°C and 450°C, were identical.

Table 3: Selected cladded (CL) and stand-alone (SA) materials for corrosion testing.

ID	Type	Cladding	Base material	Type	Cladding method	Full Thickness (mm)	Cladding Thickness (mm)	Supplier
CL02	Austenitic SS	254 SMO (31254)	P355NH / SA-516 Gr.70	Plate 300x300 mm	Explosion	12.8	3	Explomet
CL03	Austenitic SS	SS 316L (S31603)	P355NH / SA-516 Gr.70	Plate 300x300 mm	Explosion	12.8	3	Explomet
CL04	Duplex SS	Duplex 2507 (S32750)	P355NH / SA-516 Gr.70	Plate 300x300 mm	Explosion	12.8	3	Explomet
CL05	Nickel alloy	Inconel 625 (N06625)	P355NH / SA-516 Gr.70	Plate 300x300 mm	Explosion	12.8	3	Explomet
CL06	Nickel alloy	C-276 (N10276)	P355NH / SA-516 Gr.70	Plate 300x300 mm	Explosion	12.8	3	Explomet
CL09	Duplex SS	2205 (S31803)	Carbon steel	Plate 150x400 mm	Roll bonding	35	3	Industeel / ArcelorMittal
CL10	Austenitic SS	Incoloy 825 (N08825)	Carbon steel,	Plate 150x400 mm	Roll bonding	14.8	3	Industeel / ArcelorMittal
CL11	Nickel alloy	Inconel 625 (N06625)	API X65	Pipe ø342,9 mm	Metallurgical	25.2	3	Butting
SA01	Carbon steel	N/A	API K55	Pipe 13 3/8" 68lb/ft casing	N/A	12.2	N/A	LV / IDDP-1
SA05	Austenitic SS	N/A	B66 (S31266)	Pipe ø63,5x7 mm	N/A	7.0	N/A	Sandvik
SA06	Nickel alloy	N/A	Hastelloy C-22HS (N06022)	Pipe ø78,3 mm	N/A	8.6	N/A	Haynes International
SA08	Titanium	N/A	Grade 9 (R56320)	Pipe ø109,4 mm	N/A	17.4	N/A	Timet
SA10	Nickel alloy	N/A	UR 625 (N06625)	Plate 500x500 mm	N/A	10	N/A	Industeel / ArcelorMittal
SA14	Duplex SS	N/A	UR2507 (S32750)	Plate 297x210 mm	N/A	6	N/A	Industeel / ArcelorMittal
SA17	Austenitic SS	N/A	254 SMO (S31254)	Pipe ø169 mm	N/A	18	N/A	SINTEF

5.0 RESULTS

5.1 Weight loss measurements of the stand-alone samples

After testing for three weeks, sample racks were removed from the 210°C and 450°C vessels. Samples were cleaned before weighing by the procedure given in ASTM G1 (2017), based on their alloying elements. Only the Stand-Alone (SA) samples were subjected to weight-loss measurement.

Table 4: Chemical composition of the selected stand-alone materials. Values (%) are from respective standards.

	C	Mn	Cr	Ni	Mo	N	Ti	Cu	Other
API-K55	-	-	-	-	-	-	-	-	P <0.03 S <0.03
S31266	<0.03	2-4	23-25	21-24	5.2-6.2	0.35-0.6		1-2.5	W 1.5-2.5
N05022	<0.10	<0.5	20-22.5	Balance	12.5-14.5	-	-	-	Co <2.5 W 2.5-3.5 V <0.35
R56320	<0.08	-	-	-	-	<0.03	Balance	-	Al 3 V 2.5
N06625	0.03-0.10	<0.5	20-23	>58	8-10	-	< 0.4	<0.5	Nb 3.15-4.15 Co <1.0 Fe <5.0
S32750	<0.03	0.5-1.2	24.5-26.0	6-8	3-5	0.24-0.32	-	<0.5	Si 0.1-0.8
S31254	<0.02	<1.0	19.5-20	17.5-18	6-6.5	0.18-0.2	-	0.5-1	Si <0.8

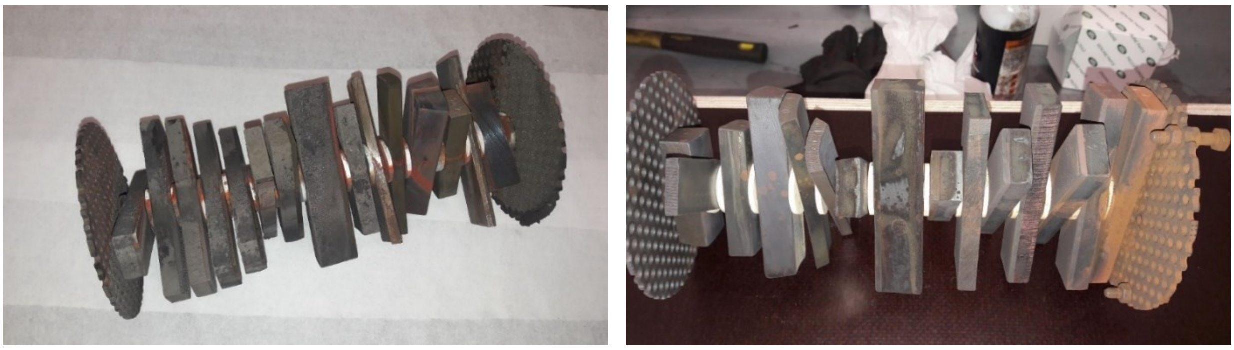

Figure 6: Samples extracted from testing at 210°C (left) and from testing at 450°C (right).

For the sample rack at 450°C, iron oxide formed on the bottom perforated plates, and the samples close to it, as can be seen in Figure 6. This is believed to be due to oxygen entering the autoclave during changing of a thermocouple. The results from weight loss measurements are used to calculate the corrosion rate as shown in Figure 7.

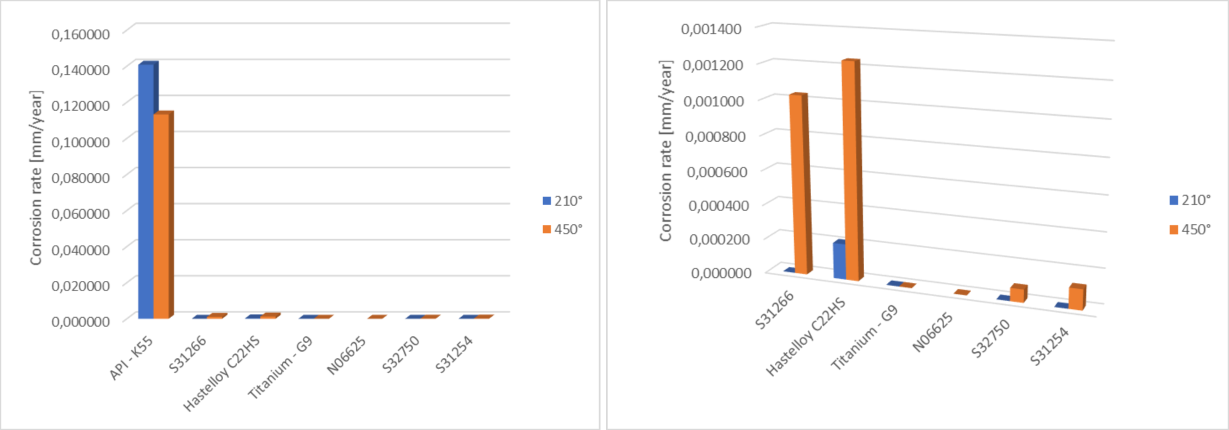

Figure 7: Measured corrosion rate for stand-alone samples. Values for N06625 at 210°C are missing.

Results from weight loss measurements show medium carbon steel API-K55, as expected, with very high corrosion rate and the only material tested to be above the commonly accepted corrosion rate of 0.1 mm/year for geothermal applications. This material shows higher corrosion rate in 210°C than 450°C, as expected due to higher risk for fluid film on the material at 210°C causing higher corrosion rate. For the Corrosion Resistant Alloys (CRA), the corrosion rate is higher for all materials in 450°C than in 210°C. For CRA alloys the protection films on the surfaces give them resistance to fluid-based surface corrosion, at higher temperatures the corrosion rate is higher. For the S31266 that is a super austenitic type with PREN value of ≈ 60, it was expected to see corrosion level close to or better than for S312254 that is lower alloyed super austenitic type with PREN $\approx$ 43. Relative high corrosion rate of N05022 (C22-HS) both in 210°C and 450°C is unexpected.

5.2 Microstructural study of the cladded materials

In Figure 8, an overview of the experimental plan for the metallurgical and microstructural examination of the cladded samples is given. Most of the samples were examined by several of the methods listed.

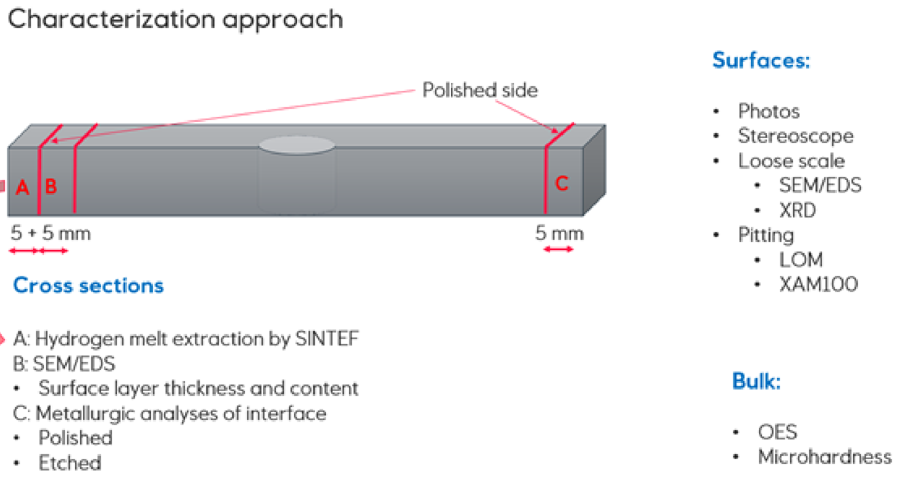

Figure 8: Overview of experimental analyses used in this work. Most of the methods where used to characterize selected and representative cladded samples.

Both representative cuts of unexposed samples and exposed coupons of the same cladded materials were closely examined by stereomicroscope before any further handling that could affect the surfaces. The surface chemistry and roughness of the starting materials will influence the interaction with the fluid during corrosion testing. This would also affect the eventual corrosion product or scale, at least at the beginning of the testing period. The clad surface of almost all the samples had rough recesses. The peak-valley distance was measured by XAM100 to be 27 µm on the sample CL04210C. This grade of roughness could also be observed on the unexposed sample CL04.

Four samples exposed at 450°C (CL03, CL04, CL05 and CL10) showed sign of pits on the surface in the examination by stereomicroscope. A part of the sample was cut, and the surface layer removed to check the cleaned surface for pits. None of the samples had growing pits visable in a stereomicroscope, and the surface looked like that of the unexposed samples.

Of interest for CRA-cladded components in hydrogen service (e.g., gaseous H_2/H_2S, H from corrosion reaction itself, from galvanic couples, cathodic protection, etc.) is the phenomenon of so-called hydrogen disbonding or dissimilar metal weld cracking. This failure mechanism is well known from different industries and applications, and can be manifested by hydrogen-induced cracking occurring exactly at the interface and at both the CRA and steel side depending on the presence of susceptible microstructures, residual and external stresses, and source of hydrogen. CRA weld claddings are typically prone to this failure mechanism due to the complex microstructural zones formed at the fusion line interface and, for example, during high temperature service (e.g., hydrogenator reactors) hydrogen would diffuse into the steel and reach saturation / steady state. However, during a shutdown situation the hydrogen would redistribute, and extremely high concentrations or spikes may occur in the austenite at the interface (Lancaster, 1999).

Table 5 summarizes all the findings from cross-sectional examinations, and it can be concluded that the clad-substrate interface flaws and defect features found (voids, porosity, inclusions and cracks) are already present in the unexposed condition and consequently originate from the manufacturing stage. The cladding defects are most significant for the explosion cladded samples and less significant for the roll-bonded samples, while the metallurgically bonded pipe samples from BUTTING are considered as sound. The presence of flaws in some of the explosion cladded steel-CRA combinations (superduplex 2507, Inconel 625 and Hastelloy C-276) may possess a risk of hydrogen trapping/accumulation/recombination and gradual disbonding.

From literature, it is known that full alpha prime precipitation is typically reached within 24 hours at 475°C and with a corresponding hardness level of 500 Vickers (Fontes et al., 2011). This alpha prime, *bcc* latticed, and chromium enriched phase would typically form by spinodal decomposition at 270°-550°C and is known to be detrimental to both the corrosion resistance and mechanical properties (so-called ‘475-degree embrittlement’).

Microhardness measurements performed in the ferrite phase of sample Cl-04 at 450°C proves that such alpha prime precipitation has indeed occurred, showing a hardness increase of about 150-200 Vickers units from about 300 to about 500 Vickers.

Table 5: Summary of cross-sectional metallographic findings in as-polished state for the cladded specimens.

Sample ID	**Unexposed**		**Exposed - 210 ºC**		**Exposed - 450 ºC**		**Concluding remarks**
	Cracks in clad	Pores/inclusions /cracks at interface	Cracks in clad	Pores/inclusions cracks at interface	Cracks in clad	Pores/inclusions /cracks at interface	
CL02 254 SMO explosion clad	No	No	No	No	No	Little	**No effect of exposure** at either temperature
CL03 SS316 explosion clad	No	Little	No	Little	One (not at interface)	Little	**No effect of exposure** at either temperature
CL04 Superduplex 2507 explosion clad	No	Yes	No	Yes	No	Yes	**No effect of exposure** at either temperature
CL05 Inconel 625 explosion clad	One crack in clad	Yes	Yes, all along interface	Yes	A few along interface	Yes	**No effect of exposure** at either temperature. Same features found in both unexposed and in both 210 & 450° C exposed conditions, although in variable amounts.
CL06 Hastelloy C-276 explosion clad	One crack in clad	Yes	No	Yes	A few along interface	Yes	
CL09 Duplex 2205 roll- bonded clad	No	No	No	No	No	Little	**No effect of exposure** at either temperature
CL10 Incoloy 825 roll-bonded clad	No	No (Intergranular etching effects from metallographic preparation?)	No	No (Intergranular etching effects from metallographic preparation?)	No	No (Intergranular etching effects from metallographic preparation?)	**No effect of exposure** at either temperature
CL11 Inconel 625 metallurgically bonded clad	No	No	No	No	No	No	**No effect of exposure** at either temperature

5.3 Hydrogen analyses of CRA-clad

To examine whether any hydrogen had been introduced into the clad layer during geothermal exposure at 210°C and 450°C for 3 weeks, the CL04-Superduplex clad was selected for melt extraction clad bulk analyses, both for the unexposed and exposed conditions. Hydrogen could enter the clad by hydrogen evolution on the clad itself or via the carbon steel. The Superduplex clad was selected because of its ferritic-austenitic microstructure allowing faster hydrogen diffusion paths in the ferrite phase compared with the austenitic alloys. In addition, the austenitic stainless steel CL02-254 SMO and the austenitic nickel-based CL11-Inconel 625 were analysed for the 450°C exposed condition.

The results are shown in Table 6. The analyses for the Superduplex clad demonstrate a consistent gradual reduction of the hydrogen bulk content following high temperature exposure for 3 weeks, being reduced to 58% and 23% of the initial hydrogen content at 210°C and 450°C, respectively. This suggests hydrogen degassing has occurred with no evidence of hydrogen charging. The hydrogen content of 450°C exposed 254 SMO and Inconel 625 clad types are both very low, in average 0.39 and 0.65 ppm, respectively.

Table 6. **Hydrogen melt extraction analysis**

Clad type	Condition	Hydrogen content [ppm]				
		Parallel 1	Parallel 2	Parallel 3	Parallel 4	Average
CL04 – Superduplex 2507	Unexposed	2.54	2.40	2.67	2.88	2.62
	210°C	1.29	1.55	1.45	1.69	1.50
	450°C	0.79	0.49	0.65	0.60	0.63
CL02 – 254 SMO	450°C	0.39	0.39	0.42	0.35	0.39
CL11 – Inconel 625	450°C	0.76	0.60	0.66	0.59	0.65

CONCLUSION

This paper describes testing of stand-alone and cladded Corrosion Resistant Alloy (CRA) on low carbon steel base material, in direct flow through geothermal steam at 210°C and 450°C. The test unit specially designed and constructed for this purpose within the GeoWell project performed well and for the first time the temperature behaviour of corrosion in the same geothermal steam at real conditions was tested.

Stand-alone samples

- For stand-alone samples it was interesting to notice that the most used casing material in geothermal steam had higher corrosion rate in 210°C than 450°C. This was not an unexpected result, and was not the result for the CRA tested where it was direct opposite that they performed better in lower temperatures.
- The higher alloyed B66 material showed higher corrosion rate at both temperatures than 254SMO, which need further attention as this was an unexpected result. In addition, the relatively high corrosion rate for C22-HS was unexpected and needs further attention.

Cladded samples

From the present characterisation of CRA-cladded samples in both the field test (210°C and 450°C in 3 weeks) and unexposed conditions, the following main conclusions can be drawn:

- Examination of as-polished metallographic samples at the steel substrate CRA-clad interface has not revealed any defects or hydrogen-induced cracks that can be associated with the field-testing exposure.
- Characterisation of the different clad types – explosion cladded, roll-bonded or metallurgically bonded – has mainly detected pre-existing manufacturing defects (voids, inclusions, cracks) for the explosion cladded samples. Most pre-existing defects have been found for the CL05-Inconel 625, CL06-Hastelloy C-276 and CL04-Superduplex 2507 explosion clad samples, while CL02-254 SMO and CL03-316SS looks sounder. The roll-bonded clad samples (CL09-22Cr duplex and CL10-Incoloy 825) have some voids and small pores along the interface, while the metallurgically bonded CL11-Inconel 625 clad sample seems defect-free and perfectly sound.
- Hydrogen melt extraction analyses of the clad bulk of CL04-Superduplex samples in both the unexposed, and 210°C and 450°C exposed conditions, showed that hydrogen was removed during field testing from an initial level of 2.6 ppm to 1.5 ppm (210°C) to 0.6 ppm (450°C). The levels of CL02-254 SMO and CL11-Inconel 625 following a 450°C exposure showed the same extremely low residual hydrogen levels (i.e., hydrogen degassing had occurred), and there is no evidence of hydrogen charging.

REFERENCES

ASTM G1-03 (2017) e1, Standard Practice for Preparing, Cleaning, and Evaluating Corrosion Test Specimens, ASTM International, West Conshohocken, PA, 2017, (www.astm.org)

Arnórsson S., Bjarnason J.Ö., Giroud N., Gunnarsson I., Stefánsson A. (2006). Sampling and analysis of geothermal fluids. *Geofluids,* **6,** 203-216.

Arnórsson S., Sigurðsson S.Þ., Svavarsson H. (1982). The chemistry of geothermal waters in Iceland. I. Calculation of aqueous speciation from 0°C to 370°C. *Geochimica et Cosmochimica Acta,* **46,** 1513-1532.

Bjarnason J.Ö. (2010). The chemical speciation program WATCH v. 2.4. Iceland GeoSurvey, Reykjavík, Iceland. 9 pp. (http://en.isor.is/sites/en.isor.is/files/download/watch_readme.pdf)

Fontes, T.F et al. Corrosion versus Mechanical Tests for indirect Detection of Alpha Prime Phase in UNS32520 Super Duplex Stainless Steel. Connosion April 2011.

Karlsdottir S.N, Thorbjornsson I.O, Corrosion Testing Down-Hole in Sour High Temperature Geothermal Well in Iceland. Proceedings of the NACE Corrosion Conference 2013, Paper 2550.

Thorbjornsson I.O, Karlsdottir S.N, Einarsson A.E, Ragnarsdottir K.R. Materials for Geothermal Steam Utilization at Higher Temperatures and Pressure. Proceedings of the World Geothermal Congress 2015, Melbourne Australia.

Lancaster, J.F. (1999). Metallurgy of Welding, Sect. 9.6 & 11.3.3, Sixth Edition, 1999.

Óskarsson F., Friðriksson Þ., Þorbjörnsson D. (2015). Geochemical monitoring of the Reykjanes geothermal reservoir 2003 to 2013. Proceedings of the World Geothermal Congress 2015, Melbourne, Australia. Paper 14085. 9 pp.